Journal of Quantitative Spectroscopy & Radiative Transfer ▮ (▮▮▮▮) ▮▮▮–▮▮▮

Contents lists available at SciVerse ScienceDirect

Journal of Quantitative Spectroscopy & Radiative Transfer

journal homepage: www.elsevier.com/locate/jqsrt

Intensities and shapes of H_2O lines in the near-infrared by tunable diode laser spectroscopy

N.H. Ngo [a], N. Ibrahim [a,b], X. Landsheere [a], H. Tran [a,*], P. Chelin [a], M. Schwell [a], J.-M. Hartmann [a]

[a] Laboratoire Interuniversitaire des Systèmes Atmosphériques (LISA, CNRS UMR 7583) Université Paris Est Créteil, Université Paris Diderot, Institut Pierre-Simon Laplace 94010 Créteil Cedex, France

[b] Institut Supérieur des Sciences Appliquées et de Technologie (ISSAT), BP 31983, Damas, Syria

ARTICLE INFO

Keywords:
Water vapor
Line-shape
Line intensity
Line broadening
Tunable diode laser spectroscopy

ABSTRACT

The integrated intensities, self- and air-broadening coefficients of thirteen transitions of $H_2^{16}O$ in the 11980–12260 cm^{-1} region, belonging to the $2\nu_1+\nu_2+\nu_3$ band, were measured. Using a tunable diode laser system, spectra were recorded at room temperature for a wide range of pressure (2–15 Torr for pure H_2O and 50–760 Torr for H_2O in air). Line parameters were adjusted from experiments using three line-shape models: the Voigt profile (VP), the (hard collision) Rautian profile (RP) and the speed dependent Voigt profile (SDVP). The results show that the RP and SDVP are in better agreement with measurements than the VP and that they lead to larger values of the line parameters (about 5% for the line broadening, and 0.8% for the line intensity). Comparisons of the present results with HITRAN 2008 [Rothman et al., JQSRT 2009, 110:533-72] show that the HITRAN intensities of the studied lines are overestimated by about 9.4%, suggesting a more complete study of the H_2O line parameters in the considered region. The Dicke narrowing and speed dependence parameters deduced from this work are also presented and discussed, demonstrating the need for a more refined line-shape model.

1. Introduction

Water vapor being a key molecule in the Earth atmosphere because of its active role in meteorology and climate, its distribution has been, for years, the target of several remote sensing experiments. The latter provide recordings of atmospheric absorption or/and emission spectra whose "inversion" yields the atmospheric humidity vertical profile. For such applications, a precise knowledge of the spectroscopic parameters (including those defining the spectral shape) of the relevant H_2O lines is obviously needed. These needs, associated with fundamental theoretical interest in the properties of the molecule and of its interaction with radiation including the effects of pressure, have motivated many spectroscopic studies. In these works, individual line parameters (e.g. position, integrated intensity, broadening coefficient, etc) are deduced from laboratory spectra assuming a specific line-shape.

For this, the Voigt profile is used in most of the available studies. Within this model, two collisional parameters are used, i.e. the Lorentz broadening and shifting coefficients, the Doppler width being generally fixed to its theoretical value. As is well known, (Refs. [1–3] and those therein), the Voigt model can lead to discrepancies with respect to measured spectra since it does not take into account two velocity effects: (a) the collision-induced velocity changes, leading to the so-called Dicke narrowing, (b) the speed dependence of the pressure-induced width and shift. Using

* Corresponding author.
E-mail address: ha.tran@lisa.u-pec.fr (H. Tran).

0022-4073/$ - see front matter © 2011 Elsevier Ltd. All rights reserved.
doi:10.1016/j.jqsrt.2011.12.007

more refined models taking into account such effects, several studies showed that the line broadening determined by the Voigt profile can be significantly underestimated, up to 10% [1,3–10], while the error is smaller for the integrated intensity, from 0.3 up to 2% [9,11]. Most of the studies, which go beyond the Voigt profile only take into account either the Dicke narrowing effect or the speed dependence of the collisional parameters while very few [1–3,7] take both into account.

The Dicke effect is usually modeled using the Galatry (soft collisions [12]) [1,3,5,6,9,11,13,14] or Rautian profile (hard collisions, [15]) [1,4–7,14,16], where the velocity changes are characterized by an empirical parameter called the velocity changing collisions frequency. For the speed dependence of the collisional parameters, a quadratic dependence on the absolute speed [10,17] or a power law dependence on the relative speed [1,3,5–7] have been used. For each approach, additional empirical parameters are then added, which describe the speed dependence of the line broadening (and shifting). Using very high quality measurements, some authors showed that one needs to take into account both of these effects for a correct fit of the experiments [1,3,7].

In this work, we have investigated 13 transitions of H_2O around 820 nm using a tunable diode-laser system. Note that the previous experimental determinations of the parameters of these transitions are all based on the Voigt profile, most of these works having used FTS spectra. In the present study, spectra have been recorded at room temperature for a wide range of pressure (2–15 Torr for pure H_2O and 50–760 Torr for H_2O in air). The spectral parameters (integrated intensities, self- and air-broadening coefficients) have been determined from fits of the recorded spectra using three line-shape models: the Voigt profile (VP), the (hard collision) Rautian profile (RP), and the speed dependent Voigt profile (SDVP).

This paper is organized as follows: Section 2 describes the experimental set-up, the measurement procedure and the line-shape models used. The results are presented and discussed in Section 3. Conclusions and future studies are in the subjects of Section 4.

2. Experimental set-up, measurement procedure and line-shape models

The experimental set-up used in this work is described in Ref. [18] where details can be found. Absorption spectra of self- and air-broadened H_2O were recorded at room temperature using an external-cavity diode laser (11300–12350 cm^{-1}). The relative calibration of the wavenumber scale was performed using a confocal Fabry–Perot etalon with the procedure described in [18]. Particular care was taken to have baseline stability during the scans, and to maximize the mode-hop free tuning range up to about 1 cm^{-1} for each investigated spectral window. Moreover, after adjusting the grating of the cavity to achieve a new wavenumber position, measurements of the diode laser output were performed using a compact grating spectrometer with a CCD-array detector (Ocean Optics, HR2000+ with 0.3 nm spectral resolution) to check that residual spontaneous emission of the external-cavity diode laser is negligible.

A White-type absorption cell with a total optical path of 40 m was used. The experiments were carried out as follows: a spectrum was first recorded with the empty cell, providing the 100% transmission reference. The cell was then filled with H_2O vapor, purified by several distillations, at pressures from 2 to 15 Torr, and self-broadened spectra were recorded. For air-broadened spectra, the cell was first filled with pure H_2O (from 4 to 7 Torr) before ambient air was added up to total pressures from 50 to 760 Torr. Partial pressures of H_2O in the mixtures were then calculated using the integrated intensity determined from the pure H_2O spectra. Pressures were measured using two capacitive pressure transducers with 10 and 1000 Torr full scale, with a stated accuracy of $\pm 0.12\%$.

Three spectral shape models have been used: the Voigt, the Rautian and the speed dependent Voigt models. The corresponding absorption coefficients for a single line are given by ([19] and references therein):

$$\alpha^{VP}(\sigma) = \frac{SP_{H_2O}}{\sqrt{\pi}}\frac{\sqrt{ln2}}{\Gamma_D} Re\{W(\sigma-\sigma_0,\Gamma_D,\Delta,\Gamma)\}, \quad (1)$$

$$\alpha^{RP}(\sigma) = \frac{SP_{H_2O}}{\sqrt{\pi}}\frac{\sqrt{ln2}}{\Gamma_D} Re\left\{\frac{W(\sigma-\sigma_0,\Gamma_D,\Delta,\Gamma+B)}{1-\sqrt{\pi}BW(\sigma-\sigma_0,\Gamma_D,\Delta,\Gamma+B)}\right\}, \quad (2)$$

$$\alpha^{SDVP}(\sigma) = \frac{SP_{H_2O}}{\pi^{3/2}}\frac{\sqrt{ln2}}{\Gamma_D} Im\left\{\int_{-\infty}^{\infty}\frac{e^{-t^2}[1-Z'(t)]}{(\sigma-\sigma_0)\frac{\sqrt{ln2}}{\Gamma_D}-t-Z(t)}dt\right\}, \quad (3)$$

where P_{H_2O} is the partial pressure of H_2O and S is the integrated intensity of the line. σ_0 and Γ_D are the unperturbed spectral position of the transition and the Doppler width. Γ, Δ and B are the collisional half-width (HWHM), the pressure induced line-shift, and the narrowing parameter. The complex probability function W is given by:

$$W(\sigma-\sigma_0,\Gamma_D,\Delta,\Gamma) = \frac{i}{\pi}\int_{-\infty}^{+\infty}\frac{e^{-t^2}}{(\sigma-\sigma_0-\Delta)\frac{\sqrt{ln2}}{\Gamma_D}-t+i\Gamma\frac{\sqrt{ln2}}{\Gamma_D}}dt. \quad (4)$$

The function $Z(t)$ and its derivative $Z'(t)$ $[dZ(t)/dt]$ in Eq. (3) are given by:

$$Z(t) = \frac{\sqrt{ln2}}{\Gamma_D}[\Delta_{col}(\tilde{\nu}t)+i\Gamma_{col}(\tilde{\nu}t)]$$

$$Z'(t) = \tilde{\nu}\frac{\sqrt{ln2}}{\Gamma_D}[\Delta'_{col}(\tilde{\nu}t)+i\Gamma'_{col}(\tilde{\nu}t)], \quad (5)$$

where $\tilde{\nu}$ ($\tilde{\nu}=\sqrt{2k_BT/m}$) is the most probable speed, $\Delta_{col}(\tilde{\nu}t)$ and $\Gamma_{col}(\tilde{\nu}t)$ being the speed dependent line shifting and broadening parameters ($\nu=\tilde{\nu}t$). In this work, the line shift is omitted in the absence of a sufficiently accurate absolute calibration of the wavenumber. In fact, the wavemeter on the apparatus has an accuracy of only 0.01 cm^{-1} while the Fabry–Perot provides the relative wavenumbers with an accuracy of a few 10^{-5} cm^{-1}. The speed dependence of the line broadening is modeled

Please cite this article as: Ngo NH, et al. Intensities and shapes of H_2O lines in the near-infrared by tunable diode laser spectroscopy. Journal of Quantitative Spectroscopy & Radiative Transfer (2012), doi:10.1016/j.jqsrt.2011.12.007

using a quadratic function [20]:

$$\Gamma_{col}(v) = \Gamma + \Gamma_2[(v/\tilde{v})^2 - 3/2], \quad (6)$$

Γ thus being the average (over velocity) collisional width $\langle \Gamma_{col}(v) \rangle$. Note that at the pressures studied in this work collisions are binary so that Γ, B and Γ_2 should show linear variations with pressure ($\Gamma = P \times \gamma$, $B = P \times \beta$ and $\Gamma_2 = P \times \gamma_2$).

3. Results and discussions

The measured spectra were least-squares fitted one-by-one with the three approaches described above and Doppler widths fixed to the theoretical values. The integrated intensity, the effective line position, the line-shape parameters (Γ, B, Γ_2) together with two parameters (straight line) describing the zero absorption level are adjusted in the fits. As expected and exemplified by Fig. 1, the VP leads to significant residuals characteristic of a line narrowing, and the RP and SDVP are in better agreement with measured spectra. This plot, and the corresponding ones for the other studied lines, show that the fit residuals obtained with the RP and SDVP are very similar and both practically within the uncertainty and noise of the measurement. At this step, our experiments thus do not enable to discriminate between these two models, forbidding any reliable conclusion on the velocity processes truly involved. On the opposite, De Vizia et al. [3] were able to show that taking into account the speed dependence effect leads to better agreement with experiment than when the Dicke narrowing is included in the line-shape. A likely explanation is the much higher quality of their measurements (signal-to-noise ratio of 15000 while ours is about 1000), which enables to unambiguously point out the small (less than 0.1%, see Fig. 3 of [3]) fit residuals obtained when only the Dicke narrowing is taken into account. Such small residuals are within the uncertainty of our measurements (cf Fig. 1). Finally, note that a slight asymmetry of the lines can also be observed in both panels of Fig. 1 (see the RP and SDVP residuals), which is probably due to the speed dependence of the pressure shift, neglected in this work. This asymmetry, which was also observed in [1,7,21], confirms that speed dependence effects do contribute to the observed line-shapes.

3.1. Integrated intensities

For the integrated intensity, only the results from pure H_2O spectra have been retained. The values obtained with the three profiles are listed in Table 1 together with one standard deviation in % (from the linear fits vs pressure). As can be seen from this table and Fig. 2a, the RP and the SDVP lead to very close values, both slightly larger (by typically 0.8%) than those determined with the VP. This result is fully consistent with those obtained in other spectral regions in Refs. [9,11].

Some of the thirteen transitions studied in this work were also measured in [18] and analyzed using the VP. However, an error in the spectra analysis procedure in that work has been detected, as explained in [22]. While comparisons between Table 1 and [18] thus cannot be made, a recent reanalysis [22] of the spectra of [18] leads to intensities very close ($\leq$ 1%) to those in Table 1.

Using our data as reference, comparisons of the line intensities obtained in this work with those from other

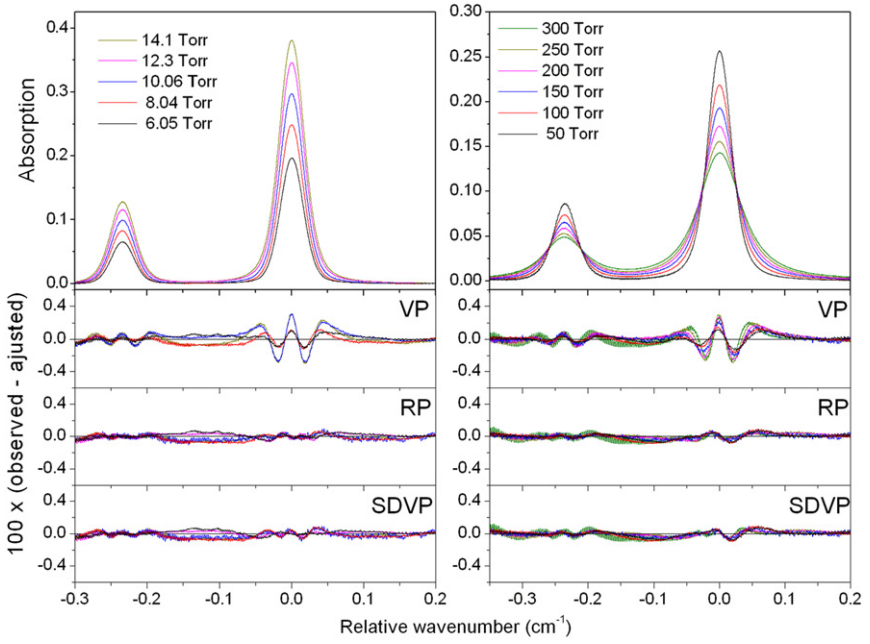

Fig. 1. Room temperature measured absorptions of the 707←606 (11988.4939 cm^{-1}) and 717←616 (11988.7257 cm^{-1}) transitions of pure water vapor (left) and of H_2O in air (right) at different pressures. The three lowest panels show the differences between measured absorptions and those adjusted using the VP, RP and SDVP.

Please cite this article as: Ngo NH, et al. Intensities and shapes of H_2O lines in the near-infrared by tunable diode laser spectroscopy. Journal of Quantitative Spectroscopy & Radiative Transfer (2012), doi:10.1016/j.jqsrt.2011.12.007

Table 1
Line intensities and self- and air-broadenings obtained using the VP, the RP and the SDVP for 13 considered transitions of H_2O. In parenthesis is one standard deviation in %. The line positions are taken from HITRAN 2008. All lines are belonging to the $2\nu_1+\nu_2+\nu_3$ band.

ν_0 (cm^{-1})	$J'K_a'K_c'$	$J''K_a''K_c''$	S (10^{-23} cm^{-1} mol^{-1} cm^2) (1δ)			γ_{self} (cm^{-1} atm^{-1}) (1δ)			γ_{air} (cm^{-1} atm^{-1}) (1δ)		
			VP	RP	SDVP	VP	RP	SDVP	VP	RP	SDVP
11988.4939	6 0 6	7 0 7	1.0626(0.5)	1.0736(0.5)	1.0764(0.6)	0.369(1.3)	0.398(1.8)	0.408(2.3)	0.06811(0.2)	0.06961(0.9)	0.06990(1.2)
11988.7257	6 1 6	7 1 7	0.3422(0.5)	0.3466(0.6)	0.3475(0.7)	0.314(1.8)	0.339(2.9)	0.344(3.8)	0.06541(0.5)	0.06738(1.2)	0.06759(1.6)
12226.1012	4 0 4	3 0 3	4.8473(0.5)	4.8586(0.5)	4.8607(0.5)	0.526(0.9)	0.534(1.1)	0.536(1.2)	0.09313(0.3)	0.09460(0.4)	0.09499(0.6)
12236.5601	5 1 5	4 1 4	4.0128(0.4)	4.0312(0.4)	4.0361(0.4)	0.475(1.3)	0.490(1.3)	0.495(1.2)	0.08497(0.2)	0.08782(0.6)	0.08907(0.5)
12244.7186	4 1 3	3 1 2	3.5084(0.4)	3.5306(0.3)	3.5515(0.4)	0.467(0.6)	0.483(0.6)	0.492(1.0)	0.08991(1.1)	0.09540(0.3)	0.09694(0.3)
12244.7881	4 3 1	3 3 0	1.0197(0.3)	1.0226(0.3)	1.0256(0.5)	0.392(1.8)	0.410(2.0)	0.426(3.8)	0.06936(0.6)	0.07719(1.3)	0.07623(1.4)
12248.5787	6 1 6	5 1 5	0.9492(1.3)	0.9528(1.3)	0.9528(1.4)	0.362(1.6)	0.374(2.3)	0.375(2.7)	0.07026(0.7)	0.07052(1.6)	0.07051(1.9)
12249.3895	6 0 6	5 0 5	2.6468(0.3)	2.6597(0.3)	2.6632(0.3)	0.429(1.2)	0.446(1.1)	0.452(1.1)	0.07630(0.6)	0.07921(0.3)	0.07987(0.6)
12259.4776	7 0 7	6 0 6	0.5645(0.1)	0.5698(0.1)	0.5709(0.1)	0.354(0.7)	0.380(0.6)	0.388(0.5)	0.06654(0.7)	0.07359(1.7)	0.07618(1.9)
12259.6033	7 1 7	6 1 6	1.6060(0.1)	1.6170(0.1)	1.6197(0.1)	0.358(0.5)	0.377(0.5)	0.383(0.6)	0.06270(0.5)	0.06446(0.7)	0.06462(1.4)
12268.9969	8 0 8	7 0 7	1.0111(0.3)	1.0210(0.2)	1.0234(0.2)	0.300(1.2)	0.325(1.3)	0.333(1.5)	0.05296(0.9)	0.05738(0.3)	0.05862(0.5)
12280.4387	6 3 4	5 3 3	0.2820(0.7)	0.2850(0.8)	0.2852(0.9)	0.389(2.5)	0.410(3.2)	0.411(3.9)	0.07538(2.0)	0.07513(3.9)	0.07480(4.6)
12280.6634	7 2 6	6 2 5	0.9262(0.3)	0.9343(0.3)	0.9359(0.3)	0.374(0.8)	0.397(1.0)	0.403(1.2)	0.07188(0.7)	0.07521(1.0)	0.07639(1.3)

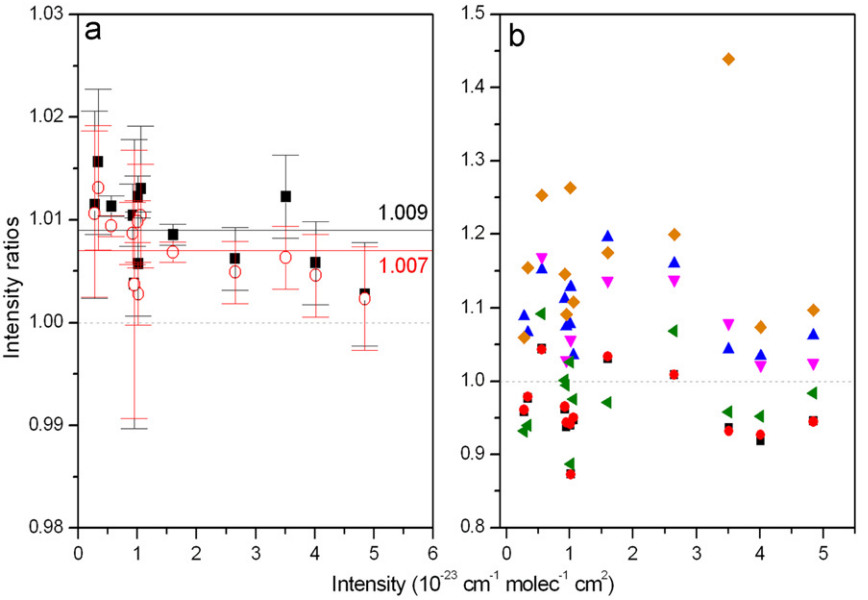

Fig. 2. (a) Ratios of the intensities of the 13 considered transitions obtained by the RP (○) and SDVP (■) to those obtained by the VP. (b) Ratios of the line intensities from [24] (▲), [25] (■), [26] (●) to our VP results and from [27] (▼), [28] (◆), [29] (◀) to our RP results (see text).

studies are shown in Fig. 2b, including those listed in the latest version of HITRAN [23], which have been provided by [24]. For the consistency of the comparisons, our VP results were retained when comparing with results of [24–26], while the RP results are compared with values of [27–29] since the latter used the modified Voigt profile. For all considered lines, our line intensities are smaller than those reported in HITRAN [23,24] with an average difference of 9.4%. Similarly, the data of [27] and [28] are on average 8.2% and 17.2% larger than our results. On the opposite, the values of [25], [26] and [29] are in good agreement with our determinations with mean differences of 4.0, 3.8 and 1.7%, respectively. The differences between these (consistent) four sets of data and those of [24,27,28] remain unexplained.

3.2. Self-broadening coefficients

The self-broadening coefficients were determined from fits of pure H_2O spectra. Fig. 3a, which displays the collisional line-widths of the 606←505 transition, shows that they have the expected linear variation with the H_2O pressure. The corresponding broadening coefficients (slopes) obtained with the VP, RP and SDVP are 0.429, 0.446 and 0.452 cm^{-1} atm^{-1}, respectively. The smaller value obtained with the VP translates (see also Fig. 4a and Table 1) the effect of the line narrowing observed in Fig. 1. The final values obtained for all lines are summarized in Table 1 and Fig. 4a.

The self-broadenings obtained in this work (using the VP for the consistency of the comparison) have been

Please cite this article as: Ngo NH, et al. Intensities and shapes of H_2O lines in the near-infrared by tunable diode laser spectroscopy. Journal of Quantitative Spectroscopy & Radiative Transfer (2012), doi:10.1016/j.jqsrt.2011.12.007

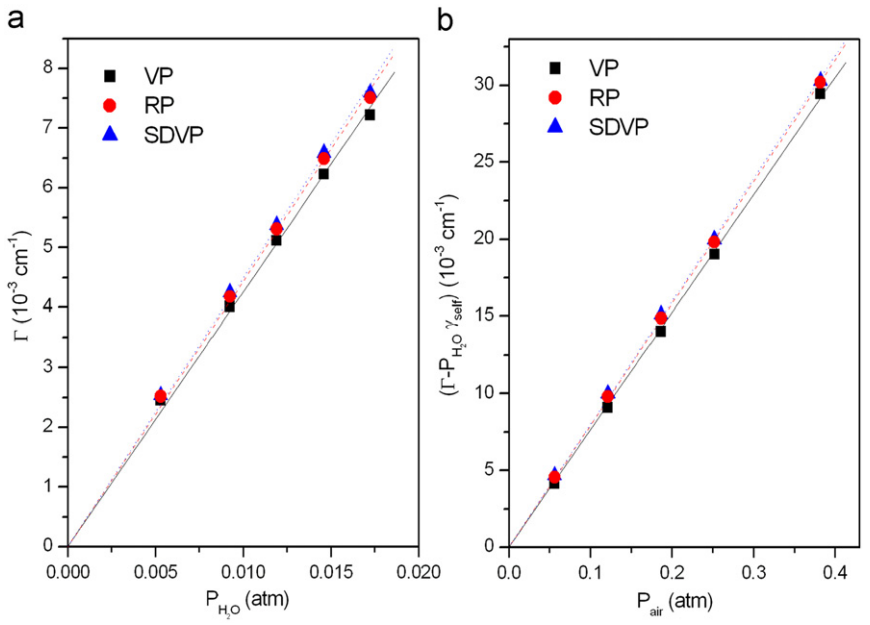

Fig. 3. Line widths of the 606←505 transition (12249.3895 cm^{-1}) as functions of the H_2O pressure (a) and air pressure (b), obtained using the VP, RP and SDVP.

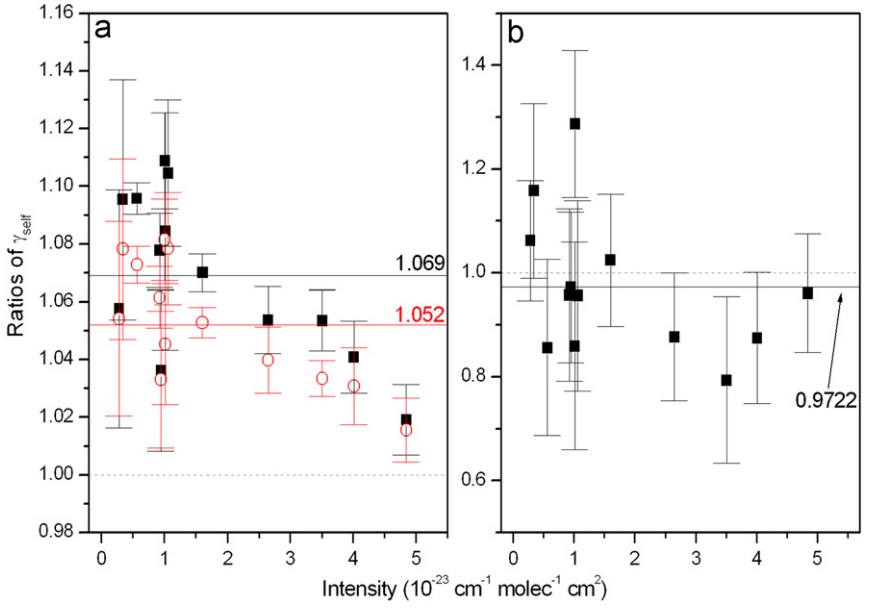

Fig. 4. (a) Ratios of the self-broadening coefficients of the 13 considered transitions obtained using the SDVP (■) and the RP (○) to those obtained by using the VP. (b) Ratios of γ_{self} provided by [24] to the present result, both obtained using the VP.

compared with the data of [24] in which FTS spectra were used. A quite good agreement is obtained, as shown by Fig. 4b. To the best of our knowledge this reference is the only one providing data to compare with ours since, as mentioned before, the values from [18] (retained in HITRAN 2008), are biased by an error in the analysis procedure [22].

3.3. Air-broadening coefficients

For spectra of H_2O diluted in ambient air, the total line-width of a transition is written as:

$$\Gamma = P_{H_2O}\gamma_{self} + P_{air}\gamma_{air}, \quad (7)$$

Please cite this article as: Ngo NH, et al. Intensities and shapes of H_2O lines in the near-infrared by tunable diode laser spectroscopy. Journal of Quantitative Spectroscopy & Radiative Transfer (2012), doi:10.1016/j.jqsrt.2011.12.007

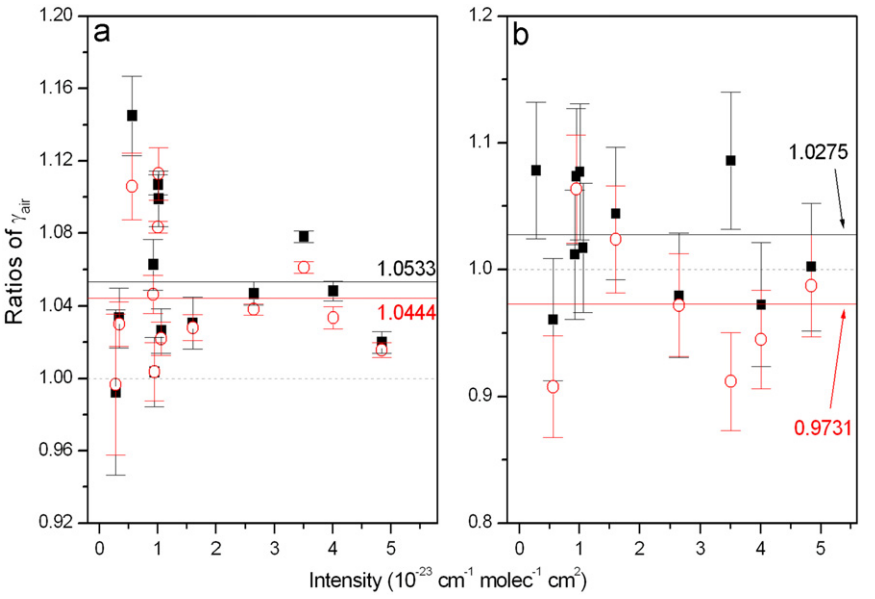

Fig. 5. (a) Ratios of the air-broadening coefficients of the 13 considered transitions obtained using the SDVP (■) and the RP (○) to those obtained by using the VP. (b) Ratios of γ_{air} from [27] (○) and from [28] (■) to the present result using the RP.

where γ_{self} and γ_{air} are, respectively, the self- and air-broadening coefficients, P_{air} is the partial pressure of air. In order to deduce γ_{air}, the partial pressure P_{H_2O} in the mixture for each spectrum was first determined from the ratio of the integrated area under the measured spectrum (obtained from fits) to the line intensity determined above. A linear fit of $(\Gamma - P_{H_2O}\gamma_{self})$ versus P_{air} then gives γ_{air}. As exemplified in Fig. 3b, the values obtained vary linearly with P_{air} and the zero value intercept at zero pressure demonstrates that the correction for self-broadening is accurate. The slopes from Fig. 3b (0.0763, 0.0792 and 0.0799 cm^{-1} atm^{-1} obtained with the VP, RP and SDVP, respectively) again demonstrate the consistency of the RP and SDVP determinations and the underestimation of the broadening by the VP (see also Fig. 5a). The values of γ_{air} for all 13 transitions are reported in Table 1.

The comparison of our air broadening parameters with the result of [27,28] (only ones available for the studied transitions) is shown in Fig. 5b. Since the latter used the modified Voigt profile to fit the measured line-shape, their results are compared with our values from the RP, for the consistency. Good agreements are obtained with both [27,28], as can be observed in Fig. 5b.

3.4. Narrowing and speed dependence parameters

The narrowing (B) and speed dependence (Γ_2) parameters of the self-broadened 606←505 transition are plotted vs pressure in Fig. 6, together with the corresponding pressure-broadened widths Γ. All show linear behaviors, the slopes of B and Γ_2 yielding the corresponding coefficients β and γ_2 of 0.0426 and 0.0243 cm^{-1} atm^{-1}. The values of β and γ_2 for all 13 lines are listed in Table 2, together with one standard deviation in percent. Note that for some transitions, the scatter is large (more than 20%, see Table 2), due to experimental uncertainties. Indeed, as

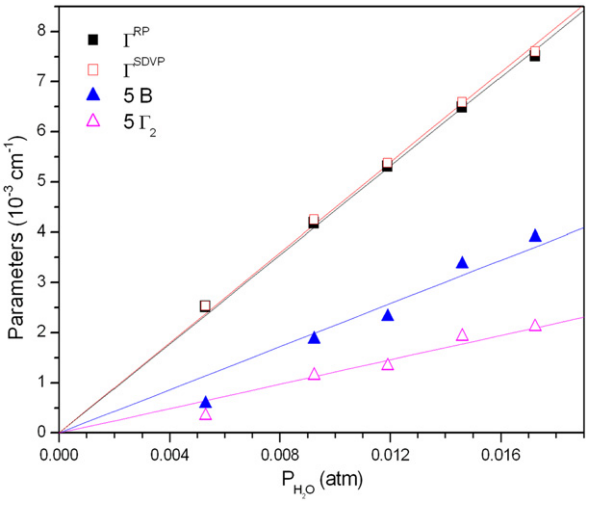

Fig. 6. Narrowing B and speed dependence Γ_2 parameters of the 606←505 transition in function of P_{H_2O} together with the corresponding pressure broadened widths Γ.

shown in Fig. 1, the line narrowing effect (shown by the residuals of the VP) is relatively small (about 1%). As a result, the β and γ_2 parameters are obtained from "subtle" line shape features of magnitude only typically ten times larger than the measurement noise and uncertainty level.

Concerning the speed dependence, our mean values[1] of γ_2 for self- and air-broadening are, respectively, of 0.028 ($\pm$0.006) and 0.011 ($\pm$0.004) cm^{-1} atm^{-1}, which correspond to 7 and 14% of the corresponding mean broadenings γ_{self} and γ_{air} determined by the SDVP. This

[1] The mean values of γ_2 and β were calculated from Table 1 retaining only values of uncertainty below 20%.

Please cite this article as: Ngo NH, et al. Intensities and shapes of H_2O lines in the near-infrared by tunable diode laser spectroscopy. Journal of Quantitative Spectroscopy & Radiative Transfer (2012), doi:10.1016/j.jqsrt.2011.12.007

Table 2
Narrowing β and speed dependence γ_2 parameters of the 13 considered transitions. In parenthesis is one standard deviation in %.

ν_0 (cm^{-1})	$J'K_a'K_c'$	$J''K_a''K_c''$	β_{self} (cm^{-1}/atm) (1δ)	β_{air} (cm^{-1}/atm) (1δ)	γ_{2self} (cm^{-1}/atm) (1δ)	γ_{2air} (cm^{-1}/atm) (1δ)
11988.4939	6 0 6	7 0 7	0.0697(10)	0.0172(13)	0.0389(13)	0.0058(18)
11988.7257	6 1 6	7 1 7	0.0397(20)	0.0131(21)	0.0208(29)	0.0046(29)
12226.1012	4 0 4	3 0 3	0.0222(18)	0.0306(23)	0.0115(26)	0.0069(21)
12236.5601	5 1 5	4 1 4	0.0399(8)	0.1043(10)	0.0220(9)	0.0136(4)
12244.7186	4 1 3	3 1 2	0.0346(5)	0.0532(10)	0.0224(8)	0.0140(3)
12244.7881	4 3 1	3 3 0	0.0490(12)	0.0243(12)	0.0307(22)	0.0071(12)
12248.5787	6 1 6	5 1 5	0.0286(22)	0.0175(10)	0.0132(33)	0.0067(13)
12249.3895	6 0 6	5 0 5	0.0426(5)	0.0292(2)	0.0243(5)	0.0093(9)
12259.4776	7 0 7	6 0 6	0.0672(4)	0.0493(15)	0.0372(3)	0.0175(7)
12259.6033	7 1 7	6 1 6	0.0465(5)	0.0141(12)	0.0260(5)	0.0051(23)
12268.9969	8 0 8	7 0 7	0.0453(9)	0.0255(3)	0.0269(10)	0.0096(4)
12280.4387	6 3 4	5 3 3	0.0370(27)	0.0168(56)	0.0164(44)	0.0053(77)
12280.6634	7 2 6	6 2 5	0.0518(9)	0.0340(7)	0.0278(11)	0.0109(8)

is in satisfactory agreement with Schneider et al. [10], who proposed a ratio γ_2/γ of 15% for H_2O in air. Note that authors of Refs. [1,3,6] used a power law vs the relative speed while we retained a quadratic law vs the absolute speed. Nevertheless, a comparison between these two approaches is possible, following Refs. [30,31]. Indeed, using Eq. (11) of [31] the values given in [1,3,6] lead to γ_2/γ of about 9 (pure H_2O) and 12% (H_2O in N_2), in good agreement with our results. Now concerning the narrowing parameter β, it can be compared to the dynamic friction coefficient β^0 deduced from the mass diffusion coefficients, using:

$$\beta^0 = \frac{k_B T}{2\pi c m D_{12}}, \tag{8}$$

where m is the H_2O molecular mass, D_{12} the mass diffusion coefficients of self-colliding or of water vapor in air. For pure H_2O, from the measured value of $D_{11}=0.17\ cm^2\ atm\ s^{-1}$ determined by [32] at room temperature, we obtain $\beta^0=0.0427\ cm^{-1}\ atm^{-1}$ while the mean value of β in Table 2 is of 0.046 ($\pm$0.014) $cm^{-1}\ atm^{-1}$. For H_2O in air, our mean value of β is 0.037 ($\pm$0.027) $cm^{-1}\ atm^{-1}$, yielding a mass diffusion coefficient of $0.20\ cm^2\ atm\ s^{-1}$. This last value is also in good agreement with the measured value of $0.220\ cm^2\ atm\ s^{-1}$ [33].

Note that one should be careful while doing such comparisons due to the large scatter of the values of β and γ_2 in Table 2. In fact, the parameters β and γ_2 deduced from our experiments depend on the considered line, which is expected for γ_2 but should not be the case for β with respect to Eqs. (2),(8). Similar to the present results, using the RP model for H_2O in N_2, Claveau and Lepère [5,6,14] found values of β ranging from 0.022 to $0.057\ cm^{-1}\ atm^{-1}$, depending on the transition. Using high signal-to-noise spectra of a single H_2O line at 1.38 μm and the Galatry profile, De Vizia et al. [3] obtained $\beta=0.139\ cm^{-1}\ atm^{-1}$ for pure H_2O. This scatter of the Dicke narrowing parameter is likely an indication that the observed profiles do not only result from velocity changes and that the speed dependence of the broadening also contributes. Considering the latter, the quadratic law vs the absolute speed used in the present work [Eq. (6)] is largely empirical and oversimplified, a statement that also applies to the alternative power law vs the relative speed used in [3], for instance. As demonstrated in Fig. 7 of Ref. [34], the speed dependence determined by this quadratic law is significantly different from that calculated using a semi-classical model [8,35]. The latter being in very good agreement with measurements including the temperature dependences of the broadening coefficient, its predictions are reliable. The "experimental" speed dependence thus seems questionable, a result further explained by the neglect of velocity changes in the SDVP profile used to fit the measurements.

These results indicate that the approaches used in this work (as in others) are probably not fully appropriate to model the line-shapes of H_2O. In fact, both velocity changes and speed dependence contribute and must be simultaneously taken into account as demonstrated in ([2] and references therein). Considering velocity changes, one must recall that the Rautian or Galatry profiles correspond to hard and soft collisions, respectively. The reality is likely in between these two extreme cases. For the speed dependence, it is also likely that the empirical models widely used (quadratic vs absolute speed or power law vs relative speed) do not well represent the true behavior. More refined approaches are thus needed. A possible direction to solve this problem might be given by the approach of Ref. [2] in which more sophisticated descriptions, largely based on theoretical predictions, of both velocity changes and speed dependences are used. Such a detailed analysis of the line-shapes of H_2O transitions is currently under study and will be presented in a forthcoming paper.

4. Conclusions

Absorption spectra of 13 transitions of H_2O near 820 nm have been accurately measured using a tunable diode laser system. Three line-shape models (VP, SDVP, RP) were used to retrieve the spectroscopic parameters from spectra fits. The SDVP and RP lead to better fits of experiments than the VP, which leads to systematic residuals and biases in the retrieved line parameters. The comparison of the present results with HITRAN [23] shows that the line intensities in this database are overestimated by about 9.4%. Nevertheless, the significant scatter of data from the various available studies calls

Please cite this article as: Ngo NH, et al. Intensities and shapes of H_2O lines in the near-infrared by tunable diode laser spectroscopy. Journal of Quantitative Spectroscopy & Radiative Transfer (2012), doi:10.1016/j.jqsrt.2011.12.007

for a new and more complete determination of the intensities of the strong lines in this spectral region. For the line-broadenings, good agreement is obtained between the present results and previous measurements. Although both the SDVP and RP are in good agreements with experiments, the retrieved narrowing and the speed dependence parameters show large scatters, which seem to indicate that these models are oversimplified. More realistic models are thus needed for which Refs. [2,36,37] give paths that deserve to be further investigated.

Acknowledgment

N. Ibrahim would like to thank the University of Paris Est Créteil (UPEC) for invitation as guest researcher in 2011.

References

[1] Lisak D, Hodges J, Ciurylo R. Comparison of semiclassical line-shape models to rovibrational H_2O spectra measured by frequency-stabilized cavity ring-down spectroscopy. Physical Review A 2006;73:012507.

[2] Tran H, Bermejo D, Domenech JL, Joubert P, Gamache RR, Hartmann JM. Collisional parameters of H_2O lines: velocity effects on the line-shape. Journal of Quantitative Spectroscopy and Radiative Transfer 2007;108:126–45.

[3] De Vizia MD, Rohart F, Castrillo A, Fasci E, Moretti L, Gianfrani L. Investigation on speed dependent effects in the near-IR spectrum of self-colliding $H_2^{18}O$ molecules. Physical Review A 2011;83:052506.

[4] Moretti L, Sasso A, Gianfrani L, Ciurylo R. Collisional-broadened and Dicke-narrowed lineshapes of $H_2^{16}O$ and $H_2^{18}O$ transitions at 1.39 μm. Journal of Molecular Spectroscopy 2001;205:20–7.

[5] Claveau C, Henry A, Hurtmans D, Valentin A. Narrowing and broadening parameters of H_2O lines perturbed by He, Ne, Ar, Kr and nitrogen in the spectral range 1850–2140 cm^{-1}. Journal of Quantitative Spectroscopy and Radiative Transfer 2001;68:273–98.

[6] Claveau C, Henry A, Lepère M, Valentin A, Hurtmans D. Narrowing and broadening parameters for H_2O lines in the ν_2 band perturbed by nitrogen from Fourier Transform and tunable diode laser spectroscopy. Journal of Molecular Spectroscopy 2002;212:171–85.

[7] Lisak D, Rusciano G, Sasso A. An accurate comparison of line-shape models on H_2O lines in the spectral region around 3 μm. Journal of Molecular Spectroscopy 2004;227:162–71.

[8] Wagner G, Birk M, Gamache RR, Hartmann JM. Collisional parameters of H_2O lines: effect of temperature. Journal of Quantitative Spectroscopy and Radiative Transfer 2005;92:211–30.

[9] Li H, Farooq A, Jeffries JB, Hanson RK. Diode laser measurements of temperature-dependent collisional-narrowing and broadening parameters of Ar-perturbed H_2O transitions at 1391.7 and 1397.8 nm. Journal of Quantitative Spectroscopy and Radiative Transfer 2008;109:132–43.

[10] Schneider M, Hase F, Blavier JF, Toon GC, Leblanc T. An empirical study on the importance of a speed-dependent Voigt line-shape model for tropospheric water vapour profile remote sensing. Journal of Quantitative Spectroscopy and Radiative Transfer 2011;112:465–74.

[11] Lisak D, Hodges JT. Low-uncertainty H_2O line intensities for the 930 nm region. Journal of Molecular Spectroscopy 2008;249:6–13.

[12] Galatry L. Simultaneous effect of Doppler and foreign gas broadening on spectral lines. Physical Review 1961;122:1218–23.

[13] Bandyopadhyay A, Ray A, Ray B, Ghosh PN. On line shape measurement and simulation of rovibrational transitions of water vapour in the infrared region. Chemical Physics Letter 2005;401:135–9.

[14] Lepère M, Henry A, Valentin A, Camy-Peyret C. Diode-laser spectroscopy: line profiles of H_2O in the region of 1.39 μm. Journal of Molecular Spectroscopy 2001;208:25–31.

[15] Rautian SG. Sobel'man II. The effect of collisions on the Doppler broadening of spectral lines. Soviet Physics Uspekhi 1967;9:701–16.

[16] Bruno A, Pesce G, Rusciano G, Sasso A. Self-, nitrogen- and oxygen-broadening coefficient measurements in the ν_1 band of H_2O using a difference frequency generation spectrometer at 3 μm. Journal of Molecular Spectroscopy 2002;215:244–50.

[17] Hodges JT, Lisak D, Lavrentieva N, Bykov A, Sinita L, Tennyson J, Barber RJ, Tolchenov RN. Comparison between theoretical calculations and high-resolution measurements of pressure broadening for near-infrared water spectra. Journal of Molecular Spectroscopy 2008;249:86–94.

[18] Ibrahim N, Chelin P, Orphal J, Baranov YI. Line parameters of H_2O around 0.8 μm studied by tuneable diode laser. Journal of Quantitative Spectroscopy and Radiative Transfer 2008;109:2523–36.

[19] Hartmann JM, Boulet C, Robert D. Collisional effects on molecular spectra. Laboratory experiments and models, consequences for applications. Amsterdam: Elsevier; 2008.

[20] Priem D, Rohart F, Colmont JM, Wlodarczak G, Bouanich JP. Line-shape study of the $J=3\leftarrow2$ rotational transition of CO perturbed by N_2 and O_2. Journal of Molecular Structure 2000;517:435–54.

[21] Grossmann BE, Browell EV. Line-shape asymmetry of water vapour absorption lines in the 720 nm wavelength region. Journal of Quantitative Spectroscopy and Radiative Transfer 1991;45:339–48.

[22] Ibrahim N, et al. Erratum to Line parameters of H2O around 0.8 μm studied by tuneable diode laser. Journal of Quantitative Spectroscopy and Radiative Transfer 2008;109:2523–36 in preparation.

[23] Rothman LS, Gordon IE, et al. The HITRAN 2008 molecular spectroscopic database. Journal of Quantitative Spectroscopy and Radiative Transfer 2009;110:533–72.

[24] Tolchenov R, Tennyson J. Water line parameters from refitted spectra constrained by empirical upper state levels: Study of the 9500–14500 cm^{-1} region. Journal of Quantitative Spectroscopy and Radiative Transfer 2008;109:559–68.

[25] Toth RA. Measurements of $H_2^{16}O$ line positions and strengths: 11610–12861 cm^{-1}. Journal ofMolecular Spectroscopy 1994:176–83.

[26] Mérienne MF, Jenouvrier A, Hermans C, Vandaele AC, Carleer M, Clerbaux C, Coheur PF, Colin R, Fally S, Bach M. Water vapor line parameters in the 13000–9250 cm^{-1} region. Journal of Quantitative Spectroscopy and Radiative Transfer 2003;82:99–117.

[27] Ponsardin PL, Browell EV. Measurements of $H_2^{16}O$ linestrengths and air-induced broadenings and shifts in the 815 nm spectral region. Journal of Molecular Spectroscopy 1997;185:58–70.

[28] Schermaul R, Learner RCM, Newham DA, Williams RG, Ballard J, Zobov NF, Belmiloud D, Tennyson J. The water vapour spectrum in the 8600–15000 cm^{-1}: experimental and theoretical studies for a new spectral line database. Journal of Molecular Spectroscopy 2001;208:32–42.

[29] Tolchenov RN, Tennyson J, Shirin SV, Zobov NF, Polyansky OL, Maurellis AN. Water line parameters for weak lines in the range 9000–12700 cm^{-1}. Journal of Molecular Spectroscopy 2003;221:99–105.

[30] D'Eu JF, Lemoine B, Rohart F. Infrared HCN lineshapes as a test of Galatry and speed dependent Voigt profiles. Journal of Molecular Spectroscopy 2002;212:96–110.

[31] Rohart F, Nguyen L, Buldyreva J, Colmont JM, Wlodarczak G. Lineshapes of the 172 and 602 GHz rotational transitions of $HC^{15}N$. Journal of Molecular Spectroscopy 2007;246:213–27.

[32] Fokin LR. Kalashnikov AN. The viscosity and self-diffusion of rarefied steam: refinement of reference data. High temperature 2008;46:614–9.

[33] Machin J. The study of evaporation from small surfaces by the direct measurement of water vapour pressure gradients. The Journal of Experimental Biology 1970;53:753–62.

[34] Ngo NH, Tran H, Gamache RR, Hartmann JM. Pressure effects on water vapor lines: beyond the Voigt profile. Philosophical Transactions of the Royal Society A 2011, accepted.

[35] Gamache RR, Hartmann JM. Collisional parameters of H_2O lines: effects of vibration. Journal of Quantitative Spectroscopy and Radiative Transfer 2004;83:119–47.

[36] Bonamy L, Tran H, Joubert P, Robert D. Memory effects in speed-changing collisions and their consequences for spectral line shape. European Physics Journal 2004;31:459–67.

[37] Tran H, Hartmann JM, Chaussard F, Gupta M. An isolated line-shape model based on the Keilson–Storer function for velocity changes II. Molecular dynamics simulations and the Q(1) lines for pure H_2. Journal of Chemical Physics 2009;131:154303.

Please cite this article as: Ngo NH, et al. Intensities and shapes of H_2O lines in the near-infrared by tunable diode laser spectroscopy. Journal of Quantitative Spectroscopy & Radiative Transfer (2012), doi:10.1016/j.jqsrt.2011.12.007